water

MDPI

Article

Valorization of Cherry By-Products as Coagulant/Flocculants Combined with Bentonite Clay for Olive Mill Wastewater Treatment

Ana R. Teixeira [1], Sílvia Afonso [2], Nuno Jorge [1], Ivo V. Oliveira [2], Berta Gonçalves [2], José A. Peres [1] and Marco S. Lucas [1,*]

[1] Centro de Química de Vila Real (CQVR), Departamento de Química, Universidade de Trás-os-Montes e Alto Douro (UTAD), Quinta de Prados, 5000-801 Vila Real, Portugal; ritamourateixeira@gmail.com (A.R.T.); njorge@uvigo.es (N.J.); jperes@utad.pt (J.A.P.)

[2] Centre for the Research and Technology for Agro-Environmental and Biological Sciences (CITAB), Institute for Innovation, Capacity Building and Sustainability of Agri-Food Production (Inov4Agro), University of Trás-os-Montes e Alto Douro (UTAD), Quinta de Prados, 5000-801 Vila Real, Portugal; safonso@utad.pt (S.A.); ivo.vaz.oliveira@utad.pt (I.V.O.); bertag@utad.pt (B.G.)

* Correspondence: mlucas@utad.pt

Abstract: In this study, two by-products resulting from the processing of cherry (stems and pits) were used as natural coagulants to promote the valorization of these wastes and treat olive mill wastewater (OMW). The efficacy of the plant-based coagulants (PBCs) in the coagulation–flocculation–decantation process (CFD) was evaluated through the removal of turbidity, total suspended solids (TSS), total polyphenols (TPh), and dissolved organic carbon (DOC). The CFD process was demonstrated to be effective in turbidity and TSS reduction in OMW. Using cherry stems (CSs), these reductions were 65.2% of turbidity and 58.0% of TSS, while cherry pits (CPs) achieved higher reductions, 78.6% of turbidity and 68.2% of TSS. To improve the effectiveness of OMW treatment, mainly regarding the removal of TPh and DOC, the CFD process was complemented with the adsorption process (using bentonite clay). The adsorption capacity of bentonite was higher in acidic conditions (pH 3.0) and, with a dosage of 3.0 g L^{-1}, reached 17.3 mg of DOC and 13.8 mg of TPh per gram of bentonite. Several adsorption isothermal models were assessed, and the Langmuir ($r^2 = 0.985$), SIPS ($r^2 = 0.992$), and Jovanovic models ($r^2 = 0.994$) provided the best fittings. According to the optimal operational conditions defined throughout the present work, the combination of CFD and adsorption removals were as follows: (1) 98.0 and 91.3% of turbidity, (2) 80.8 and 81.2% of TSS, (3) 98.1 and 97.6% of TPh and (4) 57.9 and 62.2% of DOC, for CSs and CPs, correspondingly. Overall, the results suggest that cherry by-products can be used as low-cost natural coagulants and, when combined with another natural, abundant, and cheap material, such as bentonite clay, can be a sustainable alternative for treating OMW.

Keywords: cherry stem; cherry pit; plant-based coagulants; coagulation–flocculation–decantation; adsorption process; olive oil production

Citation: Teixeira, A.R.; Afonso, S.; Jorge, N.; Oliveira, I.V.; Gonçalves, B.; Peres, J.A.; Lucas, M.S. Valorization of Cherry by-Products as Coagulant/Flocculants Combined with Bentonite Clay for Olive Mill Wastewater Treatment. *Water* **2024**, *16*, 1530. https://doi.org/10.3390/w16111530

Academic Editor: Laura Bulgariu

Received: 19 April 2024
Revised: 21 May 2024
Accepted: 24 May 2024
Published: 26 May 2024

1. Introduction

Every year, in the Mediterranean Basin, more than 2.4 million tons of olives are produced, corresponding to 95% of the total world production, and 90% of this amount is for olive oil production [1]. In 2020, Portugal produced 107.000 tons of olive oil [2]. On average, the amount of effluent generated during the olive oil extraction process is 1.2 to 1.8 m^3 per ton of olives [3]. This means that large volumes of olive mill wastewater (OMW) are generated every year, and their disposing is environmentally difficult and costly [4]. OMW is typically characterized by acidic pH, dark red to black color, foul-smelling, high

suspended solids content, high turbidity, and organic load [5,6]. The organic content is commonly constituted of reduced sugars, polyphenols, tannins, organic acids, lipids, and proteins [5], making OMW one of the most polluting effluents among agrifood industries [4,7]. Hence, the discharge of OMW without appropriate treatment causes serious environmental concerns related to the pollution of surface and groundwaters [5,6].

Due to the simplicity and efficiency of the coagulation–flocculation–decantation process (CFD), it has been widely applied to treat several types of wastewater, such as palm oil mill effluent, winery wastewater, textile wastewater, pulp mill wastewater, olive mill wastewater, and sanitary landfill leachates [8,9]. The CFD process has mostly been utilized as pre-treatment, with the aim of enhancing the quality of the treated effluent for the following stages [10,11]. CFD processes are greatly used to remove suspended solids and colloidal particles, but they can also be efficient in the removal of other components, such as pigments, organic compounds, oils, and fats [10,12]. CFD processes occur by the addition of coagulants/flocculants to wastewater, which are capable of destabilizing the colloidal materials and promoting the aggregation of small particles into large ones (flocs) followed by gravitational sedimentation and thus achieving the clearing of the effluent [6,8,13]. According to Zhao et al. [14], there are four mechanisms that can act in the coagulation–flocculation process: simple charge neutralization, charge patching, bridging, and sweeping. Several factors can affect the dominant mechanism and the efficacy of the CFD process in water/wastewater treatment, for example, the types of coagulant/flocculant agents, the amount of coagulant/flocculant, the stirring and pH conditions, and the characteristics of the liquid [6,12,14,15].

Conventional chemical-based coagulants, such as aluminum and iron salts, are the most applied in the CFD process. However, the application of these chemical agents has raised controversial issues since they have low biodegradability toxicity for living organisms and are not considered sustainable options [16]. As a result, the use of chemical coagulants has been reduced, and the search for greener and equally efficient options has increased [16,17]. Although the use of plants as natural coagulants for water treatment is an ancestral technique, it has only recently been widely studied as an alternative environmentally friendly procedure to the use of chemical-based coagulants [17–19]. Natural coagulants are biodegradable, non-toxic, non-corrosive, and cheaper than chemical coagulants [17]. They can originate from a diversity of natural sources, such as plants, marine crustaceous or shellfish, and microbial organisms [11]. According to Balbinoti et al. [10], the coagulants/flocculants are important in treating and ensuring a safe discharge of wastewater; thus, the global coagulant/flocculant market is increasing, following an annual growth rate of 5.9% in 2017 and 2022, and their economic importance justifies the study of more sustainable alternatives to chemical-based coagulants. Moreover, the agrifood industries produce massive amounts of solid and liquid by-products, so the European Union (EU) promote a zero-waste economy by 2025, drawing the attention of researchers, industries, and consumers [20].

The approach of turning wastes into raw materials allows for the reduction in the resources taken from the environment to a minimum while decreasing the waste and pollution generated. This method, known as circular economy (CE), aims to keep the materials and products in the loop as long as possible, increasing their life cycle [20]. According to the Food and Agriculture Organization of the United Nations, Portugal produced 23,930 tons of cherries during the year 2021 [2]. From this production, tons of pits/kernels, stems, and skin are wasted during cherry processing (e.g., jams, juices, and ice cream) [21–23]. Furthermore, pits signify around 14.6% of the total mass of cherries [24]. Therefore, the recovery and valorization of these by-products can be a solution to reduce the environmental and management costs and a strategy for obtaining bioactive compounds [21,23]. In general, cherries' stems in aqueous infusion have been used as diuretics, sedatives, and anti-inflammatory agents to treat urinary infections, as a traditional medicine technique, while pits are commonly used in therapeutic pillows [22]. This work proposes to implement a CE model, where the wastes of cherry processing,

stems, and pits can be forwarded and valued in the treatment of wastewater resulting from olive oil production. In Portugal, there are 6308 ha of cherry trees and 380,412 ha of olive groves (data for the year 2021 provided by Pordata [25]). These two agro-industries coexist in some regions (particularly in the North of Portugal), enabling an industrial ecology approach for a sustainable treatment solution of OMW.

Adsorption is an attractive technique to decrease or even eliminate organic and inorganic contaminants present in wastewater [26]. These contaminants are adsorbed on the external surface of the solid sorbent [12]. Thus, the search for efficient, abundant, and inexpensive adsorbent materials has increased. Clay minerals are an example of materials that have been demonstrating high potential as an adsorbent [27] due to their abundance in nature, low cost, small particle sizes (<2 μm), high surface area, which results in complex porous structure, and suitable swelling properties [27,28]. Bentonite clays are a mixture of clay minerals, predominantly montmorillonite (>60 wt.%) [29].

The main purpose of the present work was the application of agricultural by-products as natural coagulants, promoting the valorization of these materials in the treatment of OMW. This study was carried out according to the following steps: (1) characterization of cherry by-products (pits and stems), (2) application of PBC as coagulant in the CFD process and optimize the operational conditions, (3) optimization of the adsorption process with bentonite clay, and (4) evaluation of the combination of CFD with the adsorption process.

2. Materials and Methods

2.1. Reagents and Olive Mill Wastewater Sampling

Activated sodium bentonite (Na-Mt) was acquired from Angelo Coimbra & Ca., Lda (Maia, Portugal). Iron (II) sulfate heptahydrate ($FeSO_4 \bullet 7H_2O$) was acquired by Panreac (Barcelona, Spain). Sodium hydroxide (NaOH) was acquired by Labkem (Barcelona, Spain), and sulfuric acid (H_2SO_4, 95%) was purchased from Scharlau (Barcelona, Spain). The 2,2-diphenyl-1-picrylhydrazyl (DPPH), 6-hydroxy-2,5,7,8-tetramethylchroman-2-carboxylic acid (Trolox), catechin, gallic acid, and caffeic acid were all supplied by Sigma-Aldrich (Darmstadt, Germany). Nitric acid (HNO_3) and hydrogen peroxide (H_2O_2, 30% *w*/*v*) were supplied by Sigma Aldrich (St. Louis, MO, USA). Deionized water was used to prepare the respective solutions.

The OMW was collected from olive oil production in the Trás-os-Montes and Alto Douro region, northeast of Portugal. The samples were transported in plastic containers to the laboratory and stored at −40 °C until they were used.

2.2. Analytical Determinations of Olive Mill Wastewater

Numerous physicochemical parameters were measured to describe the OMW, such as chemical oxygen demand (COD), biological oxygen demand (BOD_5), dissolved organic carbon (DOC), total suspended solids (TSS), and total polyphenols (TPh). The main physicochemical parameters are shown in Table 1 (values are the average of three measurements).

Chemical oxygen demand (COD) determination was carried out in a COD reactor from Hach Co. (Loveland, CO, USA), and a Hach DR 2400 spectrophotometer (Loveland, CO, USA) was used for colorimetric measurement. Biochemical oxygen demand (BOD_5) was measured using an OxiTop system (WTW, Yellow Springs, OH, USA). Dissolved organic carbon (DOC) was determined using a Shimadzu TOC-L CSH analyzer (Shimadzu, Kyoto, Japan) coupled with an ASI-L autosampler and an NDIR detector. The turbidity was measured by a 2100N IS turbidimeter (Hach, Loveland, CO, USA), the total suspended solids (TSS) were measured using a Hach DR2400 portable spectrophotometer (Hach, Loveland, CO, USA), the pH was measured by a 3510 pH meter (Jenway, Cole-Parmer, U.K.) and conductivity was measured by a VWR C030 conductivity meter (VWR, V. Nova de Gaia, Portugal), according to the methodology of the Standard Methods [30].

The total polyphenols (TPh) was determined following the Folin–Ciocalteu method, adapted by [31]. The iron concentrations were analyzed by atomic absorption spectroscopy (AAS) using a Thermo Scientific iCE 3000 Series (Thermo Fisher Scientific, Waltham, MA, USA).

Table 1. Physicochemical characteristics of olive mill wastewater.

Parameter	OMW	
	Values	**Units**
pH	4.6 ± 0.1	Sorensen scale
Conductivity	3.8 ± 0.2	mS cm^{-1}
Turbidity	2400 ± 36	NTU
Total suspended solids—TSS	3.7 ± 0.3	g L^{-1}
Dissolved organic carbon—DOC	8.2 ± 0.1	g C L^{-1}
Chemical oxygen demand—COD	21.2 ± 0.8	g O_2 L^{-1}
Biochemical oxygen demand—BOD_5	4.0 ± 0.5	g O_2 L^{-1}
Biodegradability—BOD_5/COD	0.19 ± 0.03	-
Total polyphenols—TPh	1.5 ± 0.2	g gallic acid L^{-1}

2.3. Preparation and Characterization of Plant-Based Coagulants

Samples were collected from a 6-year-old cherry orchard (*Prunus avium* L., Lapins cultivar), grafted on Trás-os-Montes and Alto Douro region, Portugal. Fruits were harvested at the commercial ripeness stage in May 2023. Then, cherries were carried to the laboratory at the University of Trás-os-Montes and Alto Douro, Vila Real (Portugal), where stems and pits were then removed and, when necessary, lyophilized (Scanvac Coolsafe 554 Pro, Labogene, Allerød, Denmark). To finish the preparation of coagulants, cherry stems and pits were ground into a fine, dried powder using a laboratory mill (Figure 1).

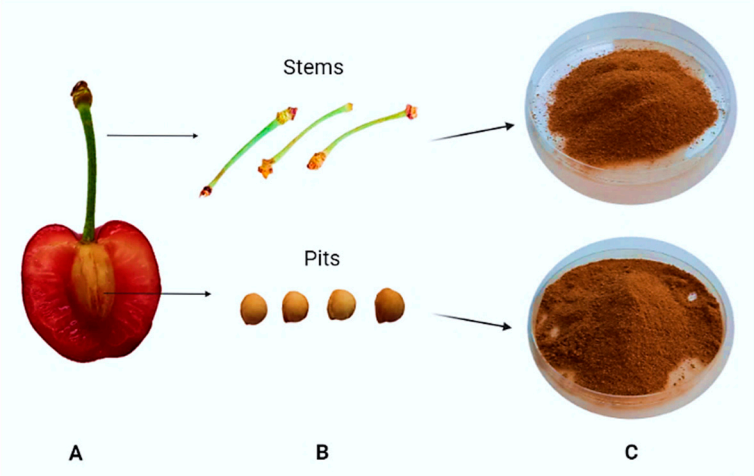

Figure 1. Cherry (**A**), cherry by-products (**B**), and plant-based powder coagulants (**C**).

2.3.1. Structural Composition of Cherry By-Products

The structural composition of cherry by-products was investigated by Fourier-transform infrared spectroscopy (FTIR) spectra, which was achieved by mixing 1 mg coagulants with 200 mg KBr. To obtain the pellets, it was necessary to insert the powder mixtures into molds and press at 10 ton cm^{-2}, which were analyzed with an IRAffinity-1S spectrometer (Shimadzu, Kyoto, Japan) and the infrared spectra in transmission mode were recorded in the 4000–400 cm^{-1} frequency region.

2.3.2. Microstructural Characterization of the Cherry By-Products

The microstructural characterization of the coagulants was carried out by scanning electron microscope (SEM/ESEM FEI QUANTA 400, Hillsboro, OR, USA). The mineral characterization of stems and cherry pits (iron, copper, sodium, potassium, calcium, and magnesium) was achieved by digestion of 500 mg of powder samples in nitric acid and hydrogen peroxide after 24 h. The samples were carried to a reactor (Techne, Cole-Parmer, U.K.) at 60 °C. The temperature of the reactor was progressively increased until it reached 150 °C. After the samples were cooled, they were added to a matrix solution (1.5 mL of HNO_3 in 1000 mL of distilled water). To finish, the cation concentrations were evaluated through atomic absorption spectroscopy (AAS) by a Thermo Scientific™ iCE™ 3000 Series (Thermo Fisher Scientific, Waltham, MA, USA).

2.3.3. Preparation of Cherry By-Product Extracts

For the bioactive composition of cherry by-products, such as total phenolics, total flavonoid, and ortho-diphenol content and antioxidant activity by the DPPH method, the preparation of the extracts was performed from the lyophilized stems and pits: 40 mg dry weight (DW) of samples were mixed with 1 mL of 70% methanol, thoroughly in a vortex. After being heated at 70 °C for 30 min and then centrifuged at 13,000 rpm, 1 °C, for 15 min, the supernatants were filtered through PTFE filters 0.2 µm, Ø 13 mm (Teknokroma, Spain) into HPLC amber vials (Chromabond 2-SVW(A) ST-CPK, Sigma-Aldrich, Tauferkichen, Germany) and stored at −20 °C until further analysis.

Total Phenolics and Total Flavonoids Content

Total phenolic content was measured according to [31,s32], with minor modifications, conducted in 96 microplate wells (Multiskan™ FC Microplate Photometer, Waltham, MA, USA): 20 µL of extract were added with 100 µL of Folin–Ciocalteu's phenol reagent (1:10 in distilled H_2O) and 80 µL of 7.5% Na_2CO_3. Then, the microplate was incubated in the dark for 15 min at 45 °C. Next, the absorbance values were recorded against a blank at 765 nm in a microplate reader (Multiskan GO Micro-plate Spectrophotometer, Thermo Scientific, Finland). Total phenolics results were expressed using a calibration curve of gallic acid standard solution as mg gallic acid equivalent (GAE) g^{-1} DW, as the mean ± standard deviation (SD) of three replicates. The total flavonoid content was measured using the spectrophotometry method adapted by [32]. In each well of a 96-well microplate, 25 µL of extract was mixed with 100 µL of ultra-pure water and 10 µL of 5% $NaNO_2$ and then placed in the dark at room temperature for 5 min. Next, 15 µL of 10% $AlCl_3$ was added and incubated at room temperature in the dark for 6 min. Then, 50 µL of NaOH 1 M and 50 µL of ultra-pure water were added. The absorbance values were measured at 510 nm against a blank. A standard curve with catechin at different concentrations was performed, and values were expressed as mg catechin equivalent (CE) g^{-1} DW, as the mean ± standard deviation (SD) of three replicates.

Quantification of Ortho-Diphenols

The method from Garcia et al. [33] was applied to determine the ortho-diphenols content, with some adaptations. A mixture of 20 µL of extract and 100 µL of ultra-pure water was performed. After that, 80 µL of phosphate buffer (pH 6.5, 0.1 M) was added to the mixture, followed by 160 µL of 5% sodium molybdate ($NaMo_2O_4 \bullet 2H_2O$) solution. After incubation for 15 min in the dark, the absorbance was measured at 370 nm against a blank reagent, and results were expressed as mg of caffeic acid equivalents (CAE) g^{-1} DW, as the mean ± standard deviation (SD) of three replicates.

Antioxidant Activity (AA)

AA was determined by 2,2-diphenyl-1-picryl-hydrazyl (DPPH) assay, according to the method of Siddhuraju and Becker [33], with minor adjustments. The assay was

conducted in a 96-well microplate, in which 15 μL of the extract was mixed with 285 μL of freshly prepared methanolic radical DPPH solution (60 μM). Microplates were incubated in the dark at room temperature for 30 min. The absorbance values were measured at 517 nm. A calibration curve with Trolox compound (Sigma-Aldrich, Germany) was performed, and the results expressed as μM Trolox equivalent g^{-1} DW as the mean ± standard deviation (SD) of three replicates.

2.4. Coagulation–Flocculation–Decantation (CFD) Experimental Setup

CFD tests were executed in a conventional model Jar-Test system (ISCO JF-4, Louisville, KY, USA), with 500 mL of effluent (OMW samples diluted 1:20, with an initial DOC of 411 mg C L^{-1}) in 1000 mL beakers at a temperature of 25 °C and a sedimentation time of 12 h. The Jar Test consisted of adding a specific coagulant dosage to the effluent under vigorous agitation (fast mix), followed by a significant reduction in agitation conditions (slow mix) to promote floc formation. Afterward, the mixture was left to sit for 12 h, and finally, the supernatant liquid was collected (decantation) [16]. The two powdered cherry by-products (stems and pits) and the ferrous iron salt were applied in the CFD process. Coagulation–flocculation–decantation process efficacy depends not only on effluent and coagulant properties, in this specific case of OMW, CSs, and CPs, but also on experimental conditions such as initial pH, coagulant dosage, particle size, temperature, mixing rate, and sedimentation time [16]. Therefore, several experiments were performed to optimize the CFD process, as described below:

1. A total of 0.1, 0.5, 1.0, and 2.0 g L^{-1} of PBCs and ferrous sulfate were added to 500 mL of OMW, and the pH varied between 3.0, 5.0, 7.0, 9.0, and 11.0;
2. After finding optimal values for the experimental conditions for pH and dosage, we followed the stirring parameter. The stirring process was studied through the variation of fast and slow mix conditions (rpm/min), respectively: 120/1, 150/2, 150/3, 180/3, and 200/2 and 20/30, 50/30, 20/20, 40/17, and 60/30.

The supernatant was withdrawn, and the parameters of turbidity, TSS, TPh, and DOC concentration were analyzed. The percentage of removal through the CFD process was determined in accordance with Equation (1) as follows:

$$X_i = \frac{C_0 - C_f}{C_0} \times 100 \quad (1)$$

where (X_i) represents turbidity, TSS, TPh, or DOC; C_0 and C_f are the initial and final concentrations, respectively.

2.5. Adsorption Experimental Setup

Several experiments were carried out, aiming to define optimal experimental conditions for the adsorption process with the bentonite clay with OMW. The adsorption process was applied as a complementary treatment to the CFD process. Initially, a concentration of 3.0 g L^{-1} of bentonite clay was added to 150 mL of diluted OMW (411 mg C L^{-1}), and the pH reaction varied between 3.0 and 9.0. The influence of bentonite dosage (1.5, 3.0, 6.0, and 10.0 g L^{-1}) was investigated following the previous practice but establishing pH = 3.0. The influence of the initial amount of organic matter on the adsorption process was evaluated by adding 3.0 g L^{-1} of bentonite clay into 150 mL (pH 3.0) of effluents with different initial DOC values (20–500 mg C L^{-1}), which were prepared from different OMW dilutions. Lastly, 3.0 g L^{-1} of bentonite clay was added to 150 mL of effluent, resulting in the CFD process, and the pH of the reaction was adjusted to 3.0.

The suspensions were stirred for 48 h (the time required to establish the equilibrium conditions). After the adsorption processes, the samples were centrifuged, and the supernatant solution was analyzed by measuring DOC and TPh values.

2.6. Statistical Analysis

All the tests were executed at least in triplicate, and the data are shown as mean value and respective standard deviation (SD). Statistical analysis was performed with SPSS software, version 24.0 (IBM Corporation, New York, NY, USA). The analysis of variance (one-way ANOVA) was the statistical tool selected to analyze all dependent variables. If a statistically significant effect was found, a comparison of mean values was performed using Tukey's multiple comparison test, with a confidence level of 95% and differences between means being considered statistically significant at ($p < 0.05$). The differences between values are represented by different letters (a, b, c, d, e).

3. Results and Discussion

3.1. Characterization of Plant-Based Coagulants Powder

The FTIR spectra were used to establish the existence of active compounds on cherry by-products. The peaks' locations are shown in Figure 2a. The first band is associated with the stretching vibration of the O-H group, demonstrating the existence of phenolic groups, proteins, and carbohydrates in CS (3416 cm^{-1}) and CP (3375 cm^{-1}) extracts [34–37]. The 2920 cm^{-1} adsorption band was observed in both by-product spectra, and they are associated with C-H stretching in the methyl and methylene groups, demonstrating the presence of phenolic acids [36]. Likewise, the peak detected at 2852 cm^{-1} in the pits spectrum is also related to the stretching symmetric vibrations of CH_3 and CH_2 functional groups, demonstrating the existence of aromatic compounds [35,36]. The peaks observed within the range 1740–1750 cm^{-1} can be attributed to the presence of carbonyl (C=O) stretching vibrations in primary amides, representing the highest intense absorption band in proteins [38]. In addition, the peaks at 1461 cm^{-1} and 1447 cm^{-1}, correspondingly to pits and stems, are ascribed to the stretching vibration of C=O in aromatic ring deformation, which can be associated with the existence of flavonoids and amino acids [36]. The peak at 1240 cm^{-1} (pits spectrum) can be assigned to C-O vibrations, displaying the existence of hydroxyflavonoids [34,36]. Furthermore, the peak observed at 1151 cm^{-1} is assigned to the C–O groups, which indicates the presence of lignin [39]. Lastly, the 1034 cm^{-1} and 1027 cm^{-1} adsorption bands are ascribed to the C-O stretching band of alcohols [36].

The SEM images (Figure 2b–e) show the microstructures of powdered stems and pits. It is observed that the cherry by-products are constituted by dark zones, which correspond to empty spaces, proving the existence of natural porosity. These porous microstructures increase the contact surface area of the coagulant powder, which results in a greater electroactive surface, causing more effective electron transfer [19].

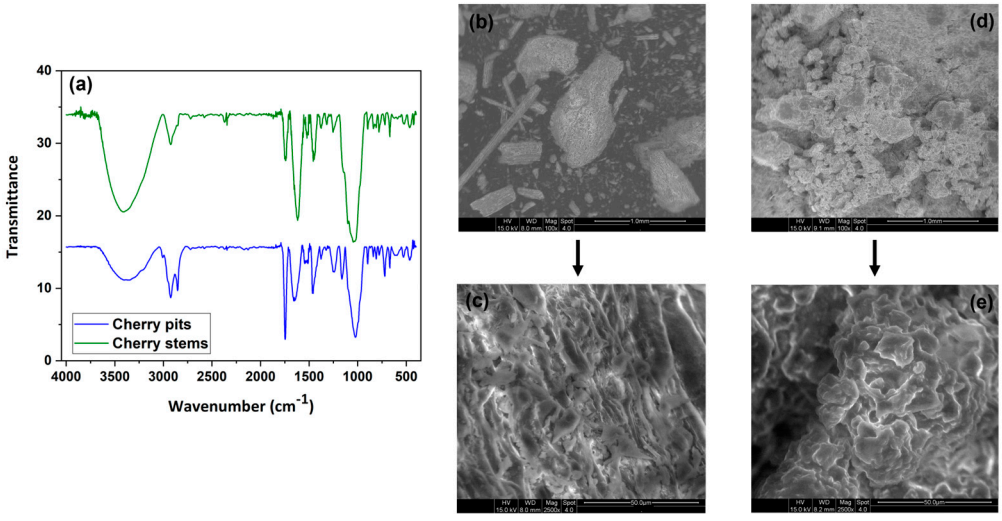

Figure 2. (**a**) FTIR spectra; SEM images of (**b**) cherry stems (100×), (**c**) cherry stems (2500×), (**d**) cherry pits (100×), and (**e**) cherry pits (2500×).

Table 2 shows the mineral characterization of the powdered coagulants. It was observed that potassium (K^+), calcium (Ca^{2+}), and magnesium (Mg^{2+}) were present in higher concentrations, followed by the microminerals, sodium (Na^+), iron (Fe^{2+}) and copper (Cu^{2+}). It was also observed that cherry stems are richer in K^+ (741.4 mg L^{-1}), Ca^{2+} (329.9 mg L^{-1}), and Na^+ (46.0 mg L^{-1}), comparatively to cherry pits. On the other hand, cherry pits had a higher content of Mg^{2+} (83.6 mg L^{-1}). Regarding the trace elements Fe^{2+} and Cu^{2+}, these were found in very similar concentrations in both by-products, around 6.1 and 0.5 mg L^{-1}, respectively. Thus, comparing the two by-products, cherry stems are richer in minerals than cherry pits. Analogous conclusions were reported by Nunes et al. [23], who studied the mineral content in the *Prunus avium L.* by-products from the Saco cultivar, namely, stems, leaves, and flowers, it was observed that of the three by-products studied, the total mineral content was higher in cherry stems.

The content of total phenolics, total flavonoids, *ortho*-diphenols, and DPPH was higher for cherry stem extract, as presented in Table 3. Significant antioxidant activity (27.88 μg Trolox g^{-1}) was found in stem extract, similar to values reported by Afonso et al. [21], concretely 28.06 μg Trolox g^{-1}. The authors also reported that the bioactive content and antioxidant activity were higher in cherry stem extract than cherry kernel extract, the same trend verified in this study, but compared with cherry pit extract.

Table 2. Mineral characterization of plant-based coagulants (expressed in mg L^{-1}).

Coagulant	K^+	Ca^{2+}	Mg^{2+}	Na^+	Fe^{2+}	Cu^{2+}
Cherry pits	342.67 ± 6.63 b	98.31 ± 10.94 b	83.60 ± 16.51 a	13.12 ± 3.84 b	6.11 ± 0.29	0.57 ± 0.04
Cherry stems	741.43 ± 29.20 a	329.88 ± 43.57 a	15.69 ± 1.79 b	45.98 ± 7.96 a	6.17 ± 0.26	0.53 ± 0.01
p-value	<0.001	<0.001	<0.001	<0.001	<0.001	<0.001

Notes: Values presented are expressed as mean ± standard deviation (SD). Mean values followed by different letters (a,b) in a column are significantly different ($p < 0.05$) according to the analysis of variance (ANOVA) and multiple range test (Tukey's test).

Table 3. Bioactive composition of cherry by-products.

Coagulant	Total Phenolics (mg GAE g^{-1})	Total Flavonoids (mg CE g^{-1})	Ortho-Diphenols (mg CAE g^{-1})	DPPH (μg Trolox g^{-1})
Cherry pits	3.59 ± 0.24 b	0.23 ± 0.03 b	0.61 ± 0.01 b	3.10 ± 0.15 b
Cherry stems	10.63 ± 0.06 a	13.98 ± 2.09 a	2.37 ± 0.11 a	27.88 ± 0.23 a
p-value	<0.001	<0.001	<0.001	<0.001

Notes: Values presented are expressed as mean ± standard deviation (SD). Mean values followed by different letters (a,b) in a column are significantly different ($p < 0.05$) according to the analysis of variance (ANOVA) and multiple range test (Tukey's test).

3.2. Coagulation–Flocculation–Decantation Experiments

3.2.1. Influence of pH

The pH conditions influence the surface charge of the coagulants because the particles can receive or give protons according to the pH [19]. Likewise, the stabilization of the suspensions is also affected by pH value [40].

To optimize the CFD process, the OMW pH varied among 3.0, 5.0, 7.0, 9.0, and 11.0. As shown in Figure 3, overall, higher efficacy of PBC is noted at pH 3.0, and for conventional coagulant (ferrous sulfate), it is at pH 9.0. The results achieved exhibit a turbidity reduction of 61.0, 65.4, and 81.3% (Figure 3a) and a TSS reduction of 53.9, 59.9, and 65.0% (Figure 3b), respectively, for CSs, CPs, and ferrous sulfate. Concerning the TPh removal (Figure 3c), for CSs, it was 2.9%, and it was 37.8% for CPs at pH 3.0. Moreover, the highest removals were 10.3% and 49.5%, observed for CSs at pH 11.0 and for CPs at pH 5.0, respectively. Regarding conventional coagulants, the TPh removals were less than 4.0% (for all studied pH conditions). These results are inconclusive regarding the most favorable pH conditions for TPh removal and can be justified for the possible influence of

iron (II) in the method quantification of TPh [41]. Lastly, regarding DOC removal (Figure 3d), almost zero removals were observed for PBC (independent of the pH), and the most significant removal for ferrous sulfate was 14.0% (pH 9.0). These DOC removals obtained from PBC can be explained by the presence of carbon compounds in their constitution; consequently, the reduction in organic matter is more difficult [19].

The proteins present in PBC (Figure 2a) are seen as possible functional agents of coagulation, with an isoelectric point varying between 10.0 and 11.0 [42]. Moreover, in pH conditions between 3.0 and 7.0, the predominant CFD mechanism is charge neutralization (proteins of the PBC with a positive charge interact with the colloidal matter with a negative charge). At pH 9.0 and 11.0, the main CFD mechanism occurs by sweeping [42]. Thus, according to the results achieved, it can be presumed that turbidity and TSS removals occurred mainly through charge neutralization. Similar conclusions were reported by Abidin et al. [43], who evaluated the use of *Jatropha curcas* seed and press cake as a coagulant in the treatment of palm oil mill wastewater. These authors reported that the best suspended solids removals occurred in acidic conditions (*Jatropha curcas* press cake at pH 1.0 and *Jatropha curcas* seed at pH 3.0). In another study, which used *Moringa oleifera* and *Jatropha curcas* as coagulants, it was observed that the amino acids present in these species are more effective in acid conditions due to the positive charges, which are dominant and behave like a cationic coagulant [44].

Regarding the removal rates obtained with ferrous sulfate, they are similar to the results obtained by Amuda and Alade [45]. In their work, they concluded that the optimum pH value was 9.0 and that the efficiency of removal was negatively influenced by the decreasing or increasing of pH conditions below or above 9.0.

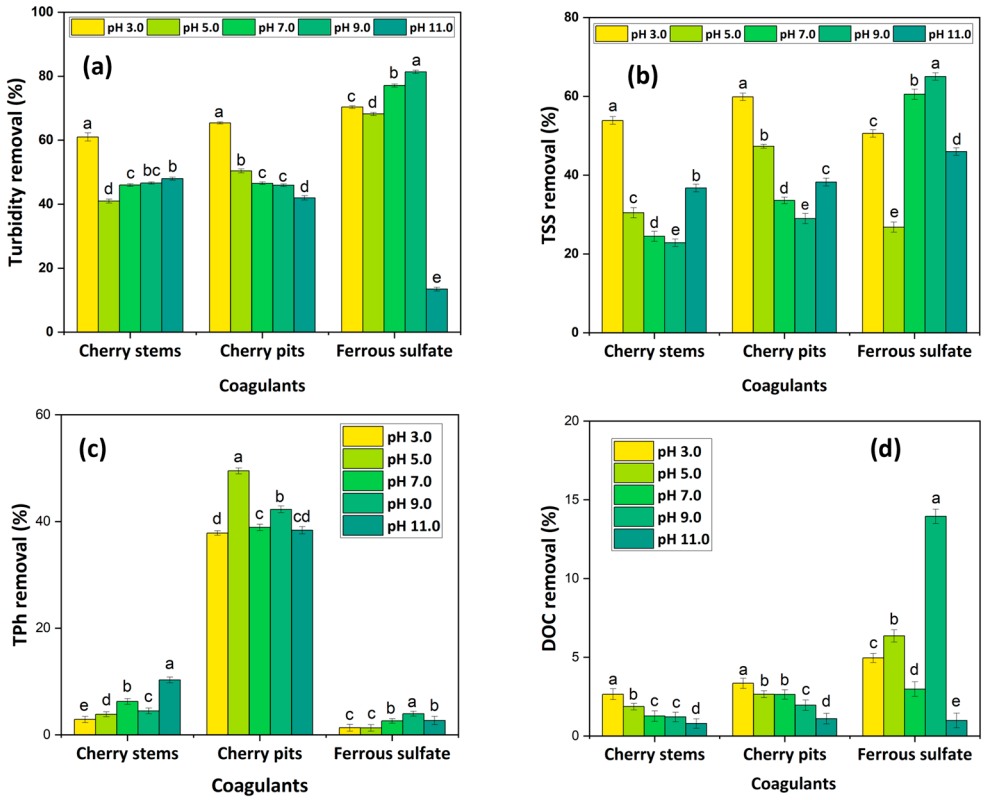

Figure 3. Influence of pH on (**a**) turbidity removal, (**b**) TSS removal, (**c**) TPh removal, and (**d**) DOC removal. Operational conditions: 1.0 g L^{-1} for each coagulant, temperature 25 °C, fast mix 150 rpm for 3 min, slow mix 20 rpm for 20 min, sedimentation time of 12 h ($[Turbidity]_0$ = 120 NTU; $[TSS]_0$ = 184 mg L^{-1}; $[TPh]_0$ = 76.2 mg gallic acid L^{-1}, $[DOC]_0$ = 411 mg O_2 L^{-1}). Values presented are expressed as mean ± standard deviation (SD). Mean values followed by different letters (a–e) in a column are significantly different ($p < 0.05$) according to the analysis of variance (ANOVA) and multiple range test (Tukey's test).

3.2.2. Coagulant Dosage Effect

The amount of coagulant is an important factor, as the use of an underdosage or overdosage can result in low performance in the CFD process [40]. On the one hand, a reduced coagulant dosage will be insufficient to destabilize or establish connections with the colloidal particles present in wastewater. Additionally, excessive use of coagulant can saturate the surface of colloids and cause particle restabilization, which eventually originates a repulsive force between colloids and thus prevents the formation of the floc [15]. To determine the most efficient coagulant dosage to perform CFD, several dosages were tested, namely 0.1, 0.5, 1.0, and 2.0 g L^{-1}. The results obtained are represented in Figure 4.

Concerning the PBC, the removal values achieved for turbidity and TSS (Figure 4a and 4b, respectively) showed a trend toward increased removal efficiency with increasing coagulant dosage. Thus, for CS coagulant, the removal values varied between 55.4 and 63.1% (turbidity) and 54.1 and 56.9% (TSS), and for CP coagulant, were around 59.7–73.7% (turbidity) and 55.9–69.1% (TSS), respectively, for 0.1 g L^{-1} and 2.0 g L^{-1}. As previously demonstrated, natural coagulants have amino acids and, when in interaction with the wastewater, suffer an ionization effect, creating carboxylate ions and protons [19]. Due to the fact that the colloidal matter present in the effluent has a negative charge, it will be attracted by the protons, originating a neutral molecule that will then flocculate and agglomerate into settleable flocs [10,19,44]. The suitable results obtained with increasing dosage can be justified by the existence of water-soluble dimeric proteins in the constitution of the CSs and CPs (noticed in FTIR analysis), which plays a role as natural polyelectrolytes with a mechanism that associates adsorption (porous structure proved by SEM images), charge neutralization, particle bridging of destabilized particles, enmeshment, and precipitation [46]. On the other hand, for TPh and DOC parameters (Figure 4c,d), it was verified that the removal values decreased with the increase in the amount of coagulant. The dosage of 0.1 g L^{-1} reached the best performance in the removal of TPh and DOC, respectively, with 42.5% and 7.76% for CSs and 44.9% and 2.11% for CPs. The reduced TPh removal with the increase in coagulant concentration (particularly CSs) can be associated with the fact that polyphenols are present in plants as secondary metabolites [41]. Similarly, in DOC reduction, as previously mentioned, higher dosages of CSs and CPs increase the concentration of carbon in the treated medium. Abidin et al. [43] reported that the optimum coagulant dosage for *Jatropha curcas* press cake was 0.14 g L^{-1}, while for *Jatropha curcas* seed was 0.12 g L^{-1}, with a turbidity reduction of 99% and 93%, respectively. Hence, the dosage of 0.1 g L^{-1} was selected for the PBC, due to the removal values achieved with this dosage and with the purpose of not introducing more carbon, which increases DOC values in the treated wastewater, as a consequent release of organic content from the natural coagulants [15].

Regarding the ferrous sulfate coagulant, the best removal values of turbidity, TSS, TPh, and DOC were obtained, respectively, with the dosage of 1.0, 1.0, 0.1, and 0.5 g L^{-1}, specifically, 81.3, 65.0, 50.6, and 16.5%. The reduction in turbidity and TSS reached its maximum with 1.0 g L^{-1} of coagulant, as dosages above this value decrease the removal efficiency due to the excess of positive charge that originates the restabilization of colloidal particles [40]. Moreover, iron salts are rapidly hydrolyzed in wastewater, originating several products, such as cationic species, which can be adsorbed by negatively charged particles and neutralize their charge; thus, an overdosing can disturb this balance [40]. The polyphenols decreased with the increase in the chemical coagulant dosage. As observed, for dosages greater than 1.0 g L^{-1}, there was practically no reduction in TPh. These values can be explained by the possible interference of iron (II) in the determination method of TPh [41]. The dosage of ferrous sulfate selected was 0.5 g L^{-1}, as it allowed us to obtain a suitable commitment, mainly in relation to DOC removal. In addition, applying higher amounts of chemical coagulant can represent a health risk due to residual quantities of excess chemical additives in treated water [47].

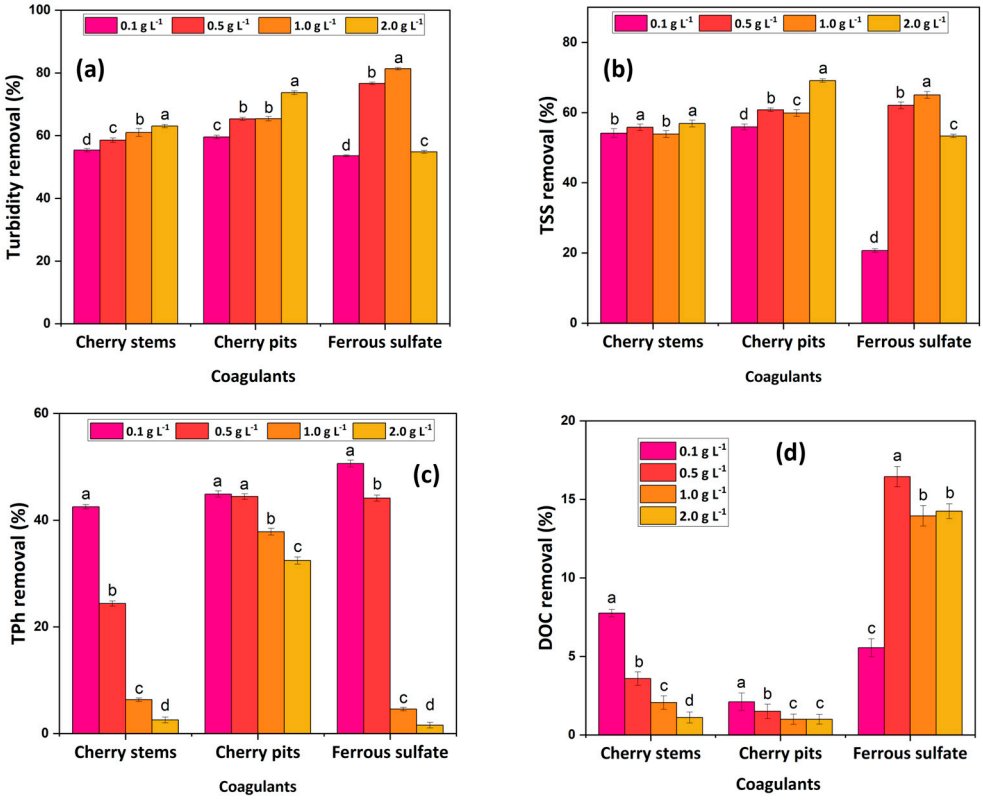

Figure 4. Development of (**a**) turbidity removal, (**b**) TSS removal, (**c**) TPh removal, and (**d**) DOC removal, testing several coagulant dosages (0.1, 0.5, 1.0, and 2.0 g L^{-1}). Experimental conditions: pH 3.0 (for PBC) and pH 9.0 (for ferrous sulfate), temperature 25 °C, fast mix 150 rpm for 3 min, slow mix 20 rpm for 20 min, sedimentation time of 12 h ($[Turbidity]_0$ = 120 NTU; $[TSS]_0$ = 184 mg L^{-1}; $[TPh]_0$ = 76.2 mg gallic acid L^{-1}, $[DOC]_0$ = 411 mg O_2 L^{-1}). Values presented are expressed as mean ± standard deviation (SD). Mean values followed by different letters (a–d) in a column are significantly different ($p < 0.05$) according to the analysis of variance (ANOVA) and multiple range test (Tukey's test).

3.2.3. Agitation Effect

In the CFD process, two stages are performed: fast and slow mix. Fast agitation disperses the coagulant throughout the wastewater to promote the destabilization of the colloidal particles (coagulation process), while slow agitation is required to promote the aggregation into flocs, getting larger and settling (flocculation process) [40,44,46,48].

This section studies the influence of the stirring process on the reduction in turbidity, TSS, TPh, and DOC from the OMW, through the variation in the mixing conditions, according to Jorge et al. [46]: (1) 120 rpm/1 min–20 rpm/30 min, (2) 150 rpm/2 min–50 rpm/30 min, (3) 150 rpm/3 min–20 rpm/20 min, (4) 180 rpm/3 min–40 rpm/17 min, and (5) 200 rpm/2 min–60 rpm/30 min, respectively, fast mix and slow mix. The results obtained (Figure 5) showed that PBC and iron sulfate were influenced by mixing conditions.

Regarding turbidity, TSS, and TPh removal, stems and pits recorded improved results using the condition (5), correspondingly, 65.2, 58.0, and 46.4% for CSs and 78.6, 68.2, and 53.3% for CPs, while for ferrous sulfate best results were observed using condition (3), 76.7% for turbidity, 62.0% for TSS, and 44.1% for TPh. For DOC removal, both CSs and ferrous sulfate presented a higher percentage of removal using condition (3), respectively, 7.76 and 16.5%, with condition (2) showing better results for CPs, 6.62%.

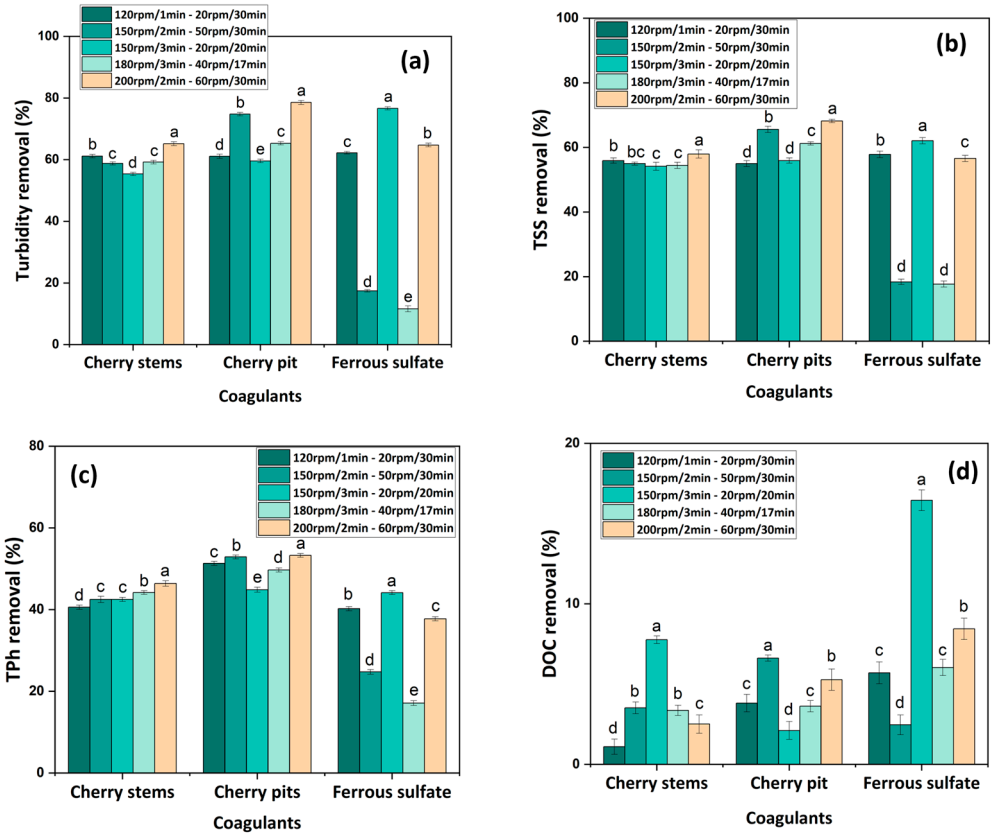

Figure 5. Evolution of (**a**) turbidity, (**b**) TSS, (**c**) TPh, and (**d**) DOC removals, testing different stirrings, fast and slow mix (rpm/min: 120/1–20/30; 150/2–50/30; 150/3–20/20; 180/3–40/17; 200/2–60/30). Experimental conditions: pH 3.0 (for PBC) and pH 9.0 (for ferrous sulfate), coagulant dosage 0.1 g L^{-1} (for PBC) and 0.5 g L^{-1} (for ferrous sulfate), temperature 25 °C, sedimentation time of 12 h ($[Turbidity]_0$ = 120 NTU; $[TSS]_0$ = 184 mg L^{-1}; $[TPh]_0$ = 76.2 mg gallic acid L^{-1}, $[DOC]_0$ = 411 mg O_2 L^{-1}). Values presented are expressed as mean ± standard deviation (SD). Mean values followed by different letters (a–e) in a column are significantly different ($p < 0.05$) according to the analysis of variance (ANOVA) and multiple range test (Tukey's test).

The coagulation can be affected by insufficient mixing, without a homogeneous distribution of the coagulant in the wastewater, or an over-mixing, due to the fact that it might break the interparticle bridging and lead to restabilization and originating an incomplete coagulation process [44]. The results obtained prove which of the coagulation–flocculation processes can be influenced by the stirring times and speed since an inappropriate agitation time will make it difficult to achieve the correct agglomeration of the colloidal particles [44].

As previously mentioned, the CFD process is widely used as pre-treatment, as it allows for the improvement of the characteristics of the effluent for further treatment stages [10,11]. In the present work, the application of the CFD process significantly reduced turbidity and TSS of OMW; however, it was less effective in removing TPh and DOC. Therefore, a complementary treatment was carried out. The adsorption process was studied in combination with the CFD process in order to increase the advantages and reach higher removal rates at low cost [12]. Bentonite clay, a natural adsorbent, was chosen for this work as it is known for its abundance, low cost, accessibility, nontoxicity, high specific surface area, high adsorption capabilities, and capacity for cation exchange [27,29,49].

3.3. Adsorption Experiments with Bentonite

3.3.1. Effect of pH

The pH conditions are a valuable parameter that interferes with the adsorption process efficiency due to controlling the surface charge properties of clay minerals [39,50]. Therefore, the capacity of activated sodium bentonite (Na-Mt) to adsorb and remove the organic contaminants from OMW was evaluated at several pH conditions (3.0–9.0); the results obtained are shown in Figure 6. Relative to the total polyphenols load, a reduction in the quantity adsorbed (from 13.8 to 4.3 mg g−1) was verified, which was a consequence of an increase in pH value from 3.0 to 9.0. The same trend was verified for TPh percentage removal, a decrease from 54.4 to 16.9% with increasing pH 3.0 to pH 9.0. Concerning DOC were verified the highest amounts adsorbed around pH 3.0–4.0 (17.3 and 17.6 mg g^{-1}), followed by a reduction in adsorbed values 13.5, 14.4, 11.2, 11.1, 12.9 mg g^{-1} at pH 5.0, 6.0, 7.0, 8.0 and 9.0). Similarly, DOC removal percentages were higher (12.6 and 12.8%) in pH 3.0–4.0, followed by smaller removals 9.8, 10.5, 8.2, 8.1, and 9.4%, varying the pH conditions between 5.0 and 9.0. These results can be ascribed to the electrostatic interactions in the adsorption process: at lower pH conditions, there is a strong electrostatic attraction between the positively charged mineral surface and the negatively charged organic matter, resulting in a high sorption affinity enabled by ligand exchange and electrostatic attraction [50]. On the contrary, the mineral surface becomes neutral or negative with the increase in pH conditions, resulting in a loss of electrostatic attraction. So, further interactions, such as hydrophobic interactions and hydrogen bonding, emerge, leading to a fragile sorption of organic matter onto the minerals.

In accordance with the results achieved, pH 3.0 was chosen as the optimum pH for the following adsorption experiments.

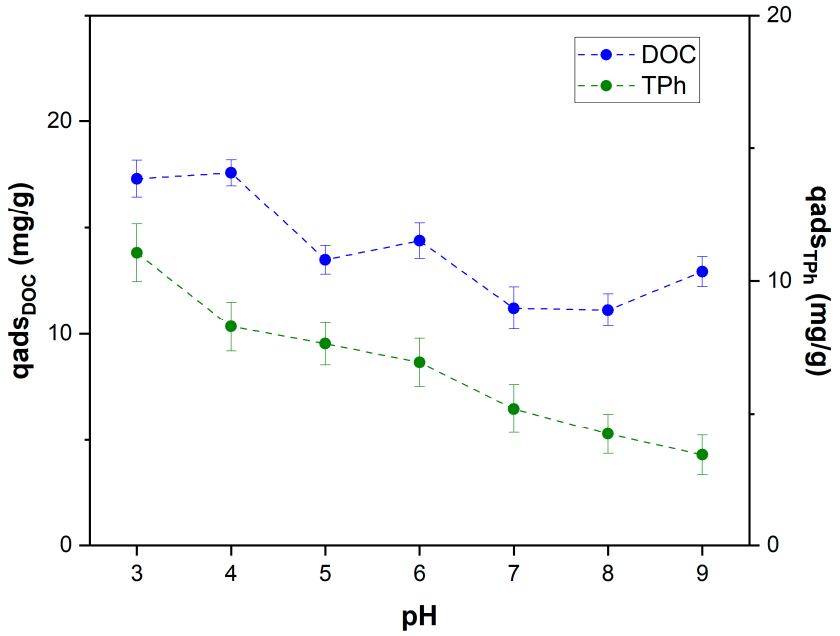

Figure 6. Adsorption of organic matter from OMW onto bentonite clay at several pH conditions (3.0–9.0). Experimental conditions: $[DOC]_0$ = 411 mg O_2 L^{-1}, $[TPh]_0$ = 76.2 mg gallic acid L^{-1}, [bentonite clay] = 3.0 g L^{-1}, volume = 150 mL, temperature 25 °C, agitation 350 rpm, time = 48 h.

3.3.2. Dosage of Bentonite Effect

The adsorption efficacy is influenced by the adsorbent amount employed since it interferes with the availability of the surface area and exchangeable sites [39]. To evaluate the effect of bentonite clay dosage on adsorption capacity, several dosages of adsorbent were tested (1.5, 3.0, 6.0, and 10 mg L^{-1}). The increase in adsorbent concentration caused

an improvement in DOC and TPh removal percentages, respectively, from 12.3 to 33.9% and 54.8 to 64.6%. However, the mass of organic content adsorbed per gram of adsorbent was reduced from 33.8 to 14.0 mg g^{-1} of DOC removal and from 27.8 to 4.9 mg g^{-1} of TPh removal (correspondingly, 1.5 and 10 g L^{-1} of adsorbent). In general, the adsorption capacity (q_{ads}) and the percentage removal show opposite behavior with increasing adsorbent dose. While the adsorption capacity decreases, the DOC and TPh removals increase. In Figure 7, a decreasing trend in the amount adsorbed (q_{ads}) at bentonite dosage is observed; thus, the adsorption capacity is higher at low dosage. Similar results were observed by [51], who stated that with a low dosage of adsorbent, the adsorption sites are more exposed to contaminants, and adsorption occurs in more extension, while with higher dosages of adsorbent, occur further empty adsorption sites, which results in a minor adsorption ability.

Considering the DOC and TPh removal proportions obtained, a bentonite dosage of 3.0 g L−1 was selected for the next steps of the adsorption process.

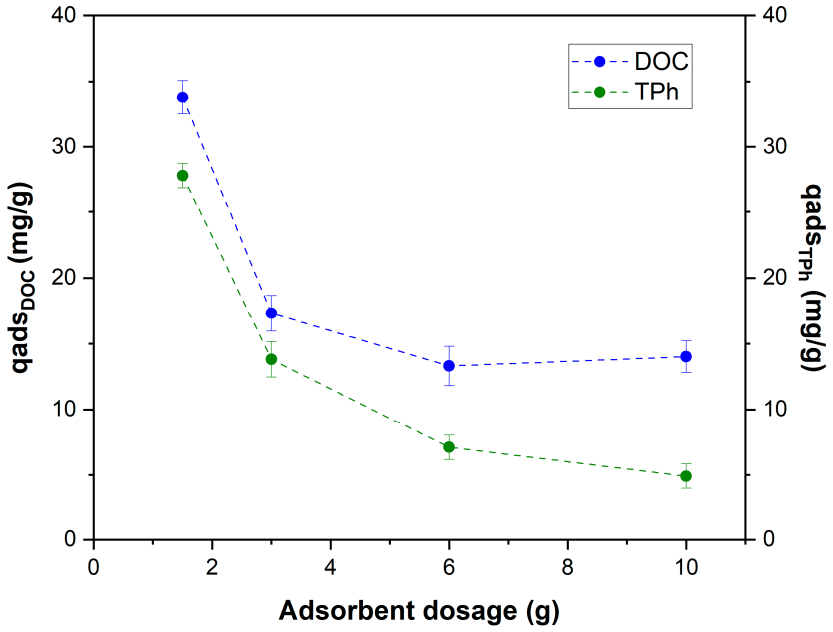

Figure 7. Adsorption of organic content from OMW onto bentonite clay at different dosages (1.5, 3.0, 6.0, and 10.0 g L^{-1}). Experimental conditions: pH 3.0, $[DOC]_0$ = 411 mg O_2 L^{-1}, $[TPh]_0$ = 76.2 mg gallic acid L^{-1}, volume = 150 mL, temperature 25 °C, agitation 350 rpm, time = 48 h.

3.3.3. Influence of DOC Initial

The initial amount of organic matter (DOC concentration) was also taken into account in the adsorption process performance with bentonite clay. The DOC values varied between 0 and 500 mg C L^{-1} according to the following experimental conditions: 3.0 g L^{-1} of Na-Mt, pH 3.0, volume = 150 mL, temperature 25 °C, and agitation at 350 rpm for 48 h. Figure 8 represents the isothermal curve related to the alteration of the adsorbed amount (q_e) as a function of the equilibrium DOC concentration. It was observed an improvement in the amount of organic carbon adsorbed (3.2 to 17.8 mg g^{-1}) with the increase in the equilibrium DOC concentration, which indicates that the gradient of concentration worked such as an increment in driving force, resulting in supplementary sorption ability [27,52].

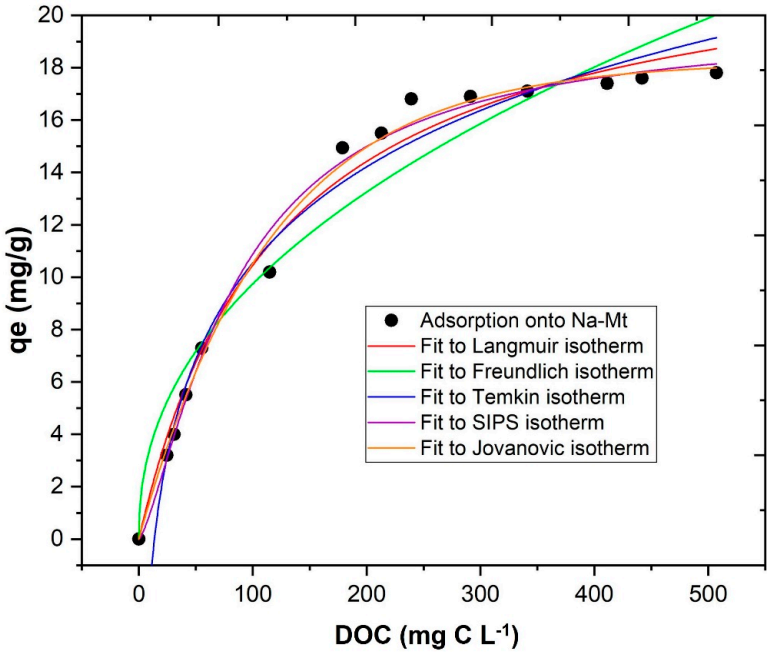

Figure 8. Adsorption isotherm describing the amount of organic matter adsorbed onto bentonite clay as a function of DOC equilibrium concentration (0–500 mg C L^{-1}). Experimental conditions: 3.0 g L^{-1} of Na-Mt, pH 3.0, volume = 150 mL, temperature 25 °C, agitation 350 rpm for 48 h.

Five different isothermal models were applied in the analysis of the experimental data achieved and were fitted to the equilibrium sorption data of organic carbon. As observed in Table 4, the Langmuir, SIPS, and Jovanovic isotherms granted the best fit to the sorption data, reflecting the regression coefficients (r^2 = 0.985, 0.992, and 0.994, respectively). The Jovanovic isotherms were developed to explain the adsorption in solid phases and consider additional interactions between the adsorbed molecules and the bulk phase [53]. Nevertheless, the Jovanovic model assumes homogeneous adsorption onto vigorously homogeneous sorption sites [27,52,53]. According to the Jovanovic model, the predicted maximum adsorption capacity (q_m), as the saturation point approaches, for this case, corresponds to 18.2 mg C g^{-1}. The adsorption affinity is measured through the binding constant (b) and corresponds to 0.009 L g^{-1}. These experimental results allowed us to evaluate and understand the removal ability of organic contaminants presented in OMW by adsorption processes with bentonite clay. According to the adsorption results obtained, the following experimental conditions were defined: volume = 150 mL, [bentonite] = 3.0 g L^{-1}, pH 3.0, temperature 25 °C, agitation 350 rpm, and time = 48 h, to apply to the combined CFD/adsorption process.

Table 4. Parameters obtained by fitting isothermal models to the bentonite adsorption data.

Isothermal Model	Equation	Model Parameters	Bentonite Adsorption
Langmuir	$q_e = \frac{q_m \times K_L \times C_e}{(1 + K_L \times C_e)}$	q_m (mg g^{-1})	23.236
		K_L (L g^{-1})	0.00818
		r^2	0.985
Freundlich	$q_e = K_F \times C_e^n$	K_f (mg g^{-1} (mg $L^{-1})^{-n}$)	1.264
		n	0.443
		r^2	0.939
SIPS	$q_e = \frac{q_m \times K_S \times C_e^n}{1 + K_S \times C_e^n}$	K_s	0.012
		q_m (mol kg^{-1})	19.794
		n	1.356
		r^2	0.992

Temkin	$q_e = \beta \times \ln K_T + \beta \times \ln C_e$	K_t (L g^{-1})	0.073
		β (J mol^{-1})	5.300
		r^2	0.981
Jovanovic	$q_e = q_m [1 - exp^{-(b \times C_e)}]$	q_m (mg g^{-1})	18.219
		b (L g^{-1})	0.009
		r^2	0.994

3.4. Combination of Coagulation–Flocculation–Decantation and Adsorption Processes

The CFD process applying cherry by-products as coagulants (stems and pits) and a chemical coagulant (ferrous sulfate) was optimized in order to reach more efficient results in OMW treatment (Section 3.2). This was followed by an adsorption process with bentonite clay, which was also optimized to obtain the best experimental conditions and, consequently, the best adsorption results (Section 3.3).

In the present step, the CFD process was associated with an adsorption process to improve removal rates in the treatment of OMW through the evaluation of four parameters, namely, turbidity, TSS, TPh, and DOC. Figure 9 shows the removals obtained by applying a combination of treatments: CFD (12 h of sedimentation/decantation) and the adsorption process (48 h of stirring).

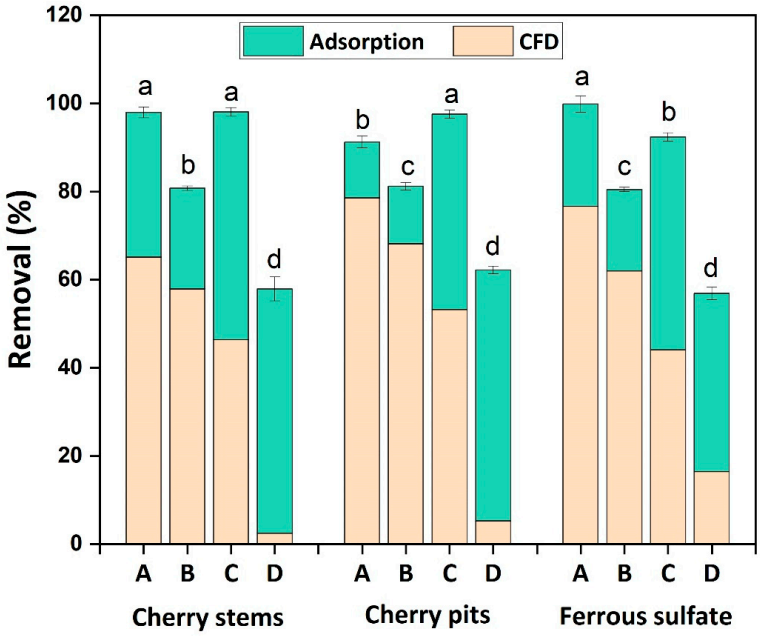

Figure 9. Final removal of (A) turbidity, (B) TSS, (C) TPh, and (D) DOC after combined processes (CFD and adsorption). Operational conditions of CFD: pH 3.0, 0.1 g L^{-1}, fast and slow mix (rpm/min) 200/2–60/30 for cherry-based coagulants; pH 9.0, 0.5 g L^{-1}, fast and slow mix (rpm/min) 150/3–20/20 for ferrous sulfate coagulant; temperature 25 °C and sedimentation time of 12 h. Experimental conditions of the adsorption process: pH 3.0, 3.0 g L^{-1} of Na-Mt, volume = 150 mL, temperature 25 °C, agitation 350 rpm for 48 h. Values presented are expressed as mean ± standard deviation (SD). Mean values followed by different letters (a–d) in a column are significantly different ($p < 0.05$) according to the analysis of variance (ANOVA) and multiple range test (Tukey's test).

The results exhibited in Figure 9 show that pre-treatment of the OMW by the CFD process was crucial to decrease turbidity and TSS.

The high reductions observed in turbidity values by the application of cherry-based coagulants in the CFD process were further increased by the adsorption process, namely, 65.2 for 98.0% (CSs) and 78.6 for 91.3% (CPs). It was noticed that in the CFD process, the

chemical coagulant (ferrous sulfate) obtained a turbidity removal less (76.7%) than that achieved by CPs (78.5%).

The final removal of TSS (CFD and adsorption) was 80.8% for CSs and 81.2% for CPs. The CFD process was responsible for 58.0% and 68.2% of this removal, respectively. It is observed that the performance of CPs (68.2%) in TSS reduction was more efficient than that of the chemical coagulant (62.1%), and a similar behavior was observed for the same coagulants in turbidity removal.

Concerning final TPh reduction, the association of treatments resulted in reductions of 98.1% (CSs), 97.6% (CPs), and 92.9% (ferrous sulfate). As previously seen, CFD treatment with PBC achieved reductions of 46.4% and 53.3% for CSs and CPs, respectively. Thus, at the end of the CFD process, using CPs, it was possible to reduce the TPh value by more than half. These results show that cherry-based coagulants can have an efficient performance on TPh removal, which is an important factor since the color in wastewater is caused by polyphenols, which can cause toxicity in the ecosystem [19].

Analyzing DOC reduction after the combined treatment processes were, correspondingly, 57.9% for CSs, 62.2% for CPs, and 56.9% for ferrous sulfate, and adsorption with bentonite was responsible for 55.4%, 56.9%, and 40.4% of this reduction, respectively. The results obtained show that the adsorption process reached higher values of DOC removal than the CFD process since cherry-based coagulants are carbon-based compounds, as previously mentioned, which makes the removal of organic matter only by CFD more difficult. However, these results also exhibit the efficacy of PBC in treating an OMW, mainly as pre-treatment in combination with adsorption.

4. Conclusions

The cherry by-products (stems and pits) were used as an alternative to chemical coagulants in the CFD process, followed by an adsorption process with bentonite clay. Overall, the results obtained prove that the combination of treatment processes, CFD and adsorption, can be efficient in the treatment of OMW. They also show that the efficiency of both treatment processes was affected by experimental conditions. According to the results achieved, it is possible to conclude the following:

- The PBC is a complex matrix. Sweet cherry by-products are carbon-based materials with amino acids, aromatic compounds, lignin, and minerals, such as potassium, calcium, and iron, in their constitution. They are rich in bioactive compounds and have antioxidant activity;
- The cherry-based coagulants achieved better performance at acidic conditions, with a concentration of 0.1 g L^{-1} and stirring conditions of 200 rpm/2 min–60 rpm/30 min. The CFD process was shown to be more efficient in the removal of turbidity and TSS, achieving 65.2 and 78.6% turbidity removal and 58.0 and 68.2% TSS removal, respectively, for CSs and CPs;
- The adsorption process with bentonite achieved high removal of DOC (12.6%) and TPh (54.4%) in pH 3.0 and with 3.0 g L^{-1}. Concerning adsorption isothermal models, the best fitting was provided by the Jovanovic model ($r^2 = 0.994$);
- The adsorption process, after the CFD process, overall, improves removal rates, despite this increase being more significant in DOC removal rates, specifically from 2.5 and 5.3% for 58.0 and 62.2% for CSs and CPs.

Overall, these results show that applying cherry by-products as coagulants, as an alternative to chemical coagulants, allows for reducing the waste that results from the cherry agro-industry and treating OMW.

Author Contributions: Conceptualization, A.R.T., S.A., and N.J.; methodology, A.R.T., S.A., I.V.O., and N.J.; validation, B.G., J.A.P., and M.S.L.; formal analysis, A.R.T.; investigation, A.R.T.; resources, B.G., J.A.P., and M.S.L.; data curation, A.R.T., S.A., and N.J.; writing—original draft preparation, A.R.T.; writing—review and editing, J.A.P. and M.S.L.; supervision, J.A.P. and M.S.L.; project

administration, J.A.P. and M.S.L.; funding acquisition, J.A.P. and M.S.L. All authors have read and agreed to the published version of the manuscript.

Funding: The authors are grateful for the financial support of Project AgriFood XXI (operation nº NORTE-01-0145-FEDER-000041) and Project OBTain (operation nº NORTE-01-0145 FEDER-000084). In addition, the authors want to thank the Portuguese Foundation for Science and Technology (FCT) for the funding provided to CQVR (UIDB/00616/2020). Ana R. Teixeira acknowledges the financial support provided by the FCT PhD grant UI/BD/150847/2020 (10.54499/UI/BD/150847/2020).

Data Availability Statement: Data are contained within the article.

Acknowledgments: The authors want to acknowledge CITAB (UIDB/04033/2020), also supported by FCT. The authors are also grateful for the support provided by the Unidade de Microscopia Eletrónica (UME) of UTAD.

Conflicts of Interest: The authors declare no conflicts of interest.

References

1. Solomakou, N.; Goula, A.M. Treatment of Olive Mill Wastewater by Adsorption of Phenolic Compounds. *Rev. Environ. Sci. Biotechnol.* **2021**, *20*, 839–863. https://doi.org/10.1007/s11157-021-09585-x.
2. FAOSTAT Data. Available online: https://www.fao.org/faostat/en/#data/QCL (accessed on 22 September 2023).
3. Lee, Z.S.; Chin, S.Y.; Lim, J.W.; Witoon, T.; Cheng, C.K. Treatment Technologies of Palm Oil Mill Effluent (POME) and Olive Mill Wastewater (OMW): A Brief Review. *Environ. Technol. Innov.* **2019**, *15*, 100377. https://doi.org/10.1016/j.eti.2019.100377.
4. Donner, M.; Erraach, Y.; López-i-Gelats, F.; Manuel-i-Martin, J.; Yatribi, T.; Radić, I.; El Hadad-Gauthier, F. Circular Bioeconomy for Olive Oil Waste and By-Product Valorisation: Actors' Strategies and Conditions in the Mediterranean Area. *J. Environ. Manag.* **2022**, *321*, 115836. https://doi.org/10.1016/j.jenvman.2022.115836.
5. Esteves, B.M.; Rodrigues, C.S.D.; Maldonado-Hódar, F.J.; Madeira, L.M. Treatment of High-Strength Olive Mill Wastewater by Combined Fenton-like Oxidation and Coagulation/Flocculation. *J. Environ. Chem. Eng.* **2019**, *7*, 103252. https://doi.org/10.1016/j.jece.2019.103252.
6. Domingues, E.; Fernandes, E.; Gomes, J.; Castro-Silva, S.; Martins, R.C. Olive Oil Extraction Industry Wastewater Treatment by Coagulation and Fenton's Process. *J. Water Process Eng.* **2021**, *39*, 101818. https://doi.org/10.1016/j.jwpe.2020.101818.
7. García, C.A.; Hodaifa, G. Real Olive Oil Mill Wastewater Treatment by Photo-Fenton System Using Artificial Ultraviolet Light Lamps. *J. Clean. Prod.* **2017**, *162*, 743–753. https://doi.org/10.1016/j.jclepro.2017.06.088.
8. Lee, C.S.; Robinson, J.; Chong, M.F. A Review on Application of Flocculants in Wastewater Treatment. *Process Saf. Environ. Prot.* **2014**, *92*, 489–508. https://doi.org/10.1016/j.psep.2014.04.010.
9. Jorge, N.; Teixeira, A.R.; Matos, C.C.; Lucas, M.S.; Peres, J.A. Combination of Coagulation–Flocculation–Decantation and Ozonation Processes for Winery Wastewater Treatment. *Int. J. Environ. Res. Public Health* **2021**, *18*, 8882.
10. Balbinoti, J.R.; Junior, R.E.S.; Sousa, L.B.F.; Bassetti, F.d.J.; Balbinoti, T.C.V.; Jorge, L.M.M.; Jorge, R.M.M. Plant-Based Coagulants for Food Industry Wastewater Treatment. *J. Water Process Eng.* **2023**, *52*, 103525. https://doi.org/10.1016/j.jwpe.2023.103525.
11. Ang, W.L.; Mohammad, A.W. State of the Art and Sustainability of Natural Coagulants in Water and Wastewater Treatment. *J. Clean. Prod.* **2020**, *262*, 121267. https://doi.org/10.1016/j.jclepro.2020.121267.
12. Badawi, A.K.; Zaher, K. Hybrid Treatment System for Real Textile Wastewater Remediation Based on Coagulation/Flocculation, Adsorption and Filtration Processes: Performance and Economic Evaluation. *J. Water Process Eng.* **2021**, *40*, 101963. https://doi.org/10.1016/j.jwpe.2021.101963.
13. Vuppala, S.; Shaik, R.U.; Stoller, M. Multi-Response Optimization of Coagulation and Flocculation of Olive Mill Wastewater: Statistical Approach. *Appl. Sci.* **2021**, *11*, 2344. https://doi.org/10.3390/app11052344.
14. Zhao, C.; Zhou, J.; Yan, Y.; Yang, L.; Xing, G.; Li, H.; Wu, P.; Wang, M.; Zheng, H. Application of Coagulation/Flocculation in Oily Wastewater Treatment: A Review. *Sci. Total Environ.* **2021**, *765*, 142795. https://doi.org/10.1016/j.scitotenv.2020.142795.
15. Bahrodin, M.B.; Zaidi, N.S.; Hussein, N.; Sillanpää, M.; Prasetyo, D.D.; Syafiuddin, A. Recent Advances on Coagulation-Based Treatment of Wastewater: Transition from Chemical to Natural Coagulant. *Curr. Pollut. Reports* **2021**, *7*, 379–391. https://doi.org/10.1007/s40726-021-00191-7.
16. Maurya, S.; Daverey, A. Evaluation of Plant-Based Natural Coagulants for Municipal Wastewater Treatment. *3 Biotech* **2018**, *8*, 77. https://doi.org/10.1007/s13205-018-1103-8.
17. Saritha, V.; Karnena, M.K.; Dwarapureddi, B.K. "Exploring Natural Coagulants as Impending Alternatives towards Sustainable Water Clarification"—A Comparative Studies of Natural Coagulants with Alum. *J. Water Process Eng.* **2019**, *32*, 100982. https://doi.org/10.1016/j.jwpe.2019.100982.
18. Martins, R.B.; Jorge, N.; Lucas, M.S.; Raymundo, A.; Barros, A.I.R.N.A.; Peres, J.A. Food By-Product Valorization by Using Plant-Based Coagulants Combined with AOPs for Agro-Industrial Wastewater Treatment. *Int. J. Environ. Res. Public Health* **2022**, *19*, 4134.
19. Hamam, M.; Chinnici, G.; Di Vita, G.; Pappalardo, G.; Pecorino, B.; Maesano, G.; D'Amico, M. Circular Economy Models in Agro-Food Systems: A Review. *Sustainability* **2021**, *13*, 3453. https://doi.org/10.3390/su13063453.

20. Afonso, S.; Oliveira, I.V.; Meyer, A.S.; Aires, A.; Saavedra, M.J.; Gonçalves, B. Phenolic Profile and Bioactive Potential of Stems and Seed Kernels of Sweet Cherry Fruit. *Antioxidants* **2020**, *9*, 1295. https://doi.org/10.3390/antiox9121295.
21. Nunes, A.R.; Gonçalves, A.C.; Falcão, A.; Alves, G.; Silva, L.R. *Prunus avium* L. (Sweet Cherry) by-Products: A Source of Phenolic Compounds with Antioxidant and Anti-Hyperglycemic Properties—A Review. *Appl. Sci.* **2021**, *11*, 8516. https://doi.org/10.3390/app11188516.
22. Nunes, A.R.; Gonçalves, A.C.; Pinto, E.; Amaro, F.; Flores-Félix, J.D.; Almeida, A.; de Pinho, P.G.; Falcão, A.; Alves, G.; Silva, L.R. Mineral Content and Volatile Profiling of *Prunus avium* L. (Sweet Cherry) By-Products from Fundão Region (Portugal). *Foods* **2022**, *11*, 751. https://doi.org/10.3390/foods11050751.
23. Mateus, A.R.S.; Pena, A.; Sendón, R.; Almeida, C.; Nieto, G.A.; Khwaldia, K.; Silva, A.S. By-Products of Dates, Cherries, Plums and Artichokes: A Source of Valuable Bioactive Compounds. *Trends Food Sci. Technol.* **2023**, *131*, 220–243. https://doi.org/10.1016/j.tifs.2022.12.004.
24. INE Estatística Sobre Portugal e Europa. Available online: https://www.pordata.pt/portugal/superficie+das+principais+arvores+de+fruto+e+oliveiras-3365 (accessed on 20 August 2023).
25. Vieira, Y.; Netto, M.S.; Lima, É.C.; Anastopoulos, I.; Oliveira, M.L.S.; Dotto, G.L. An Overview of Geological Originated Materials as a Trend for Adsorption in Wastewater Treatment. *Geosci. Front.* **2022**, *13*, 101150. https://doi.org/10.1016/j.gsf.2021.101150.
26. Guimarães, V.; Lucas, M.S.; Peres, J.A. Combination of Adsorption and Heterogeneous Photo-Fenton Processes for the Treatment of Winery Wastewater. *Environ. Sci. Pollut. Res.* **2019**, *26*, 31000–31013.
27. Zhou, Y.; Lu, J.; Zhou, Y.; Liu, Y. Recent Advances for Dyes Removal Using Novel Adsorbents: A Review. *Environ. Pollut.* **2019**, *252*, 352–365. https://doi.org/10.1016/j.envpol.2019.05.072.
28. Vezentsev, A.I.; Gorbunova, N.M.; Sokolovskiy, P.V.; Mar'inskikh, S.G.; Chub, A.V.; Chau, N.H.; Greish, A.A. On the Adsorption Mechanism of Copper Ions on Bentonite Clay. *Russ. Chem. Bull.* **2022**, *71*, 651–655. https://doi.org/10.1007/s11172-022-3461-y.
29. APHA; AWWA; WEF. *Standard Methods for the Examination of Water and Wastewater*; 20th ed American Public Health Association; American Water Works Association; Water Environment Federation: Washington, DC, USA; Denver, CO, USA; Alexandria, VA, USA, 1999; ISBN 0875532357.
30. Singleton, V.L.; Rossi, J.A. Colorimetry of Total Phenolics with Phosphomolybdic-Phosphotungstic Acid Reagents. *Am. J. Enol. Vitic.* **1965**, *16*, 144–158.
31. Dewanto, V.; Wu, X.; Adom, K.K.; Liu, R.H. Thermal Processing Enhances the Nutritional Value of Tomatoes by Increasing Total Antioxidant Activity. *J. Agric. Food Chem.* **2002**, *50*, 3010–3014. https://doi.org/10.1021/jf0115589.
32. Garcia, B.; Coelho, J.; Costa, M.; Pinto, J.; Paiva-Martins, F. A Simple Method for the Determination of Bioactive Antioxidants in Virgin Olive Oils. *J. Sci. Food Agric.* **2013**, *93*, 1727–1732. https://doi.org/10.1002/jsfa.5958.
33. Siddhuraju, P.; Becker, K. Antioxidant Properties of Various Solvent Extracts of Total Phenolic Constituents from Three Different Agroclimatic Origins of Drumstick Tree *(Moringa oleifera* Lam.) Leaves. *J. Agric. Food Chem.* **2003**, *51*, 2144–2155. https://doi.org/10.1021/jf020444+.c
34. Kashyap, P.; Riar, C.S.; Jindal, N. Optimization of Ultrasound Assisted Extraction of Polyphenols from Meghalayan Cherry Fruit (*Prunus Nepalensis*) Using Response Surface Methodology (RSM) and Artificial Neural Network (ANN) Approach. *J. Food Meas. Charact.* **2021**, *15*, 119–133. https://doi.org/10.1007/s11694-020-00611-0.
35. Cruz-Lopes, L.; Dulyanska, Y.; Domingos, I.; Ferreira, J.; Fragata, A.; Guiné, R.; Esteves, B. Influence of Pre-Hydrolysis on the Chemical Composition of *Prunus Avium* Cherry Seeds. *Agronomy* **2022**, *12*, 280.
36. Siejak, P.; Smułek, W.; Nowak-Karnowska, J.; Dembska, A.; Neunert, G.; Polewski, K. Bird Cherry (*Prunus padus*) Fruit Extracts Inhibit Lipid Peroxidation in PC Liposomes: Spectroscopic, HPLC, and GC–MS Studies. *Appl. Sci.* **2022**, *12*, 7820. https://doi.org/10.3390/app12157820.
37. Jorge, N.; Teixeira, A.R.; Lucas, M.S.; Peres, J.A. Agro-Industrial Wastewater Treatment with Acacia Dealbata Coagulation/Flocculation and Photo-Fenton-Based Processes. *Recycling* **2022**, *7*, 54. https://doi.org/10.3390/recycling7040054.
38. ELsayed, E.M.; Nour El-Den, A.A.; Elkady, M.F.; Zaatout, A.A. Comparison of Coagulation Performance Using Natural Coagulants against Traditional Ones. *Sep. Sci. Technol.* **2021**, *56*, 1779–1787. https://doi.org/10.1080/01496395.2020.1795674.
39. Pap, S.; Radonić, J.; Trifunović, S.; Adamović, D.; Mihajlović, I.; Vojinović Miloradov, M.; Turk Sekulić, M. Evaluation of the Adsorption Potential of Eco-Friendly Activated Carbon Prepared from Cherry Kernels for the Removal of Pb^{2+}, Cd^{2+} and Ni^{2+} from Aqueous Wastes. *J. Environ. Manag.* **2016**, *184*, 297–306. https://doi.org/10.1016/j.jenvman.2016.09.089.
40. Saritha, V.; Srinivas, N.; Srikanth Vuppala, N.V. Analysis and Optimization of Coagulation and Flocculation Process. *Appl. Water Sci.* **2017**, *7*, 451–460. https://doi.org/10.1007/s13201-014-0262-y.
41. Chen, L.-Y.; Cheng, C.-W.; Liang, J.-Y. Effect of Esterification Condensation on the Folin-Ciocalteu Method for the Quantitative Measurement of Total Phenols. *Food Chem.* **2015**, *170*, 10–15. https://doi.org/10.1016/j.foodchem.2014.08.038.
42. Jorge, N.; Teixeira, A.R.; Lucas, M.S.; Peres, J.A. Enhancement of EDDS-Photo-Fenton Process with Plant-Based Coagulants for Winery Wastewater Management. *Environ. Res.* **2023**, *229*, 116021. https://doi.org/10.1016/j.envres.2023.116021.
43. Abidin, Z.Z.; Madehi, N.; Yunus, R. Coagulative Behaviour of *Jatropha curcas* and Its Performance in Wastewater Treatment. *Environ. Prog. Sustain. Energy* **2017**, *36*, 1709–1718. https://doi.org/10.1002/ep.12635.
44. Owodunni, A.A.; Ismail, S. Revolutionary Technique for Sustainable Plant-Based Green Coagulants in Industrial Wastewater Treatment—A Review. *J. Water Process Eng.* **2021**, *42*, 102096. https://doi.org/10.1016/j.jwpe.2021.102096.

45. Amuda, O.S.; Alade, A. Coagulation/Flocculation Process in the Treatment of Abattoir Wastewater. *Desalination* **2006**, *196*, 22–31. https://doi.org/10.1016/j.desal.2005.10.039.
46. Jorge, N.; Teixeira, A.R.; Lucas, M.S.; Peres, J.A. Combined Organic Coagulants and Photocatalytic Processes for Winery Wastewater Treatment. *J. Environ. Manag.* **2023**, *326*, 116819. https://doi.org/10.1016/j.jenvman.2022.116819.
47. Amuda, O.S.; Amoo, I.A. Coagulation/Flocculation Process and Sludge Conditioning in Beverage Industrial Wastewater Treatment. *J. Hazard. Mater.* **2007**, *141*, 778–783. https://doi.org/10.1016/j.jhazmat.2006.07.044.
48. Kenea, D.; Denekew, T.; Bulti, R.; Olani, B.; Temesgen, D.; Sefiw, D.; Beyene, D.; Ebba, M.; Mekonin, W. Investigation on Surface Water Treatment Using Blended Moringa Oleifera Seed and Aloe Vera Plants as Natural Coagulants. *S. Afr. J. Chem. Eng.* **2023**, *45*, 294–304. https://doi.org/10.1016/j.sajce.2023.06.005.
49. Muslim, W.A.; Al-nasri, S.K.; Albayati, T.M.; Salih, I.K. Investigation of Bentonite Clay Minerals as a Natural Adsorbents for Cs-137 Real Radioactive Wastewater Treatment. *Desalin. Water Treat.* **2024**, *317*, 100121. https://doi.org/10.5772/intechopen.72352.
50. Zhao, T.; Xu, S.; Hao, F. Differential Adsorption of Clay Minerals: Implications for Organic Matter Enrichment. *Earth-Sci. Rev.* **2023**, *246*, 104598. https://doi.org/10.1016/j.earscirev.2023.104598.
51. El Azzouzi, L.; El Aggadi, S.; Ennouhi, M.; Ennouari, A.; Kabbaj, O.K.; Zrineh, A. Removal of the Amoxicillin Antibiotic from Aqueous Matrices by Means of an Adsorption Process Using Kaolinite Clay. *Sci. Afr.* **2022**, *18*, e01390. https://doi.org/10.1016/j.sciaf.2022.e01390.
52. Teixeira, A.R.; Jorge, N.; Fernandes, J.R.; Lucas, M.S.; Peres, J.A. Textile Dye Removal by *Acacia Dealbata Link*. Pollen Adsorption Combined with UV-A/NTA/Fenton Process. *Top. Catal.* **2022**, *65*, 1045–1061. https://doi.org/10.1007/s11244-022-01655-w.
53. Jovanović, D.S. Physical Adsorption of Gases-I: Isotherms for Monolayer and Multilayer Adsorption. *Kolloid-Zeitschrift Zeitschrift für Polym.* **1969**, *235*, 1203–1213. https://doi.org/10.1007/BF01542530.